Observation and Characterization of the $CH_3S(O)CH^-$ and $CH_3S(O)CH^-\cdot H_2O$ Carbene Anions by Photoelectron Imaging and Photofragment Spectroscopy

Luis Velarde,[†] Terefe Habteyes,[‡] Richard S. Glass, and Andrei Sanov*

Department of Chemistry, University of Arizona, Tucson, Arizona 85721-0041

Received: December 22, 2008; Revised Manuscript Received: February 6, 2009

We report the observation of the $CH_3S(O)CH^-$ and $CH_3S(O)CH^-\cdot H_2O$ carbene anions formed upon overall H_2^+ abstraction from dimethyl sulfoxide by O^-. Photoelectron spectroscopy reveals singlet and triplet carbenes for the remaining neutral, with the singlet state assigned as the ground state. Although some formation of the distonic $CH_2S(O)CH_2^-$ radical anion is also expected, no conclusive evidence of the presence of this isomer is found. The photoelectron spectrum of $HCSO^-$ is also reported for the first time. Photofragmentation of $CH_3S(O)CH^-$ with 532 nm light reveals two main types of anionic products: a dominant $HCSO^-$ fragment, resulting from methyl elimination, and a less intense SO^- product. For the monohydrated anion, an additional $SO^-\cdot H_2O$ fragment is observed. Intriguingly, both the $SO^-\cdot H_2O$ and SO^- products are produced with much higher yields in the fragmentation of $CH_3S(O)CH^-\cdot H_2O$, compared to the SO^- yield from the dissociation of the bare $CH_3S(O)CH^-$ anion. Two possible pathways are proposed as likely mechanisms for the SO^--based photoproducts, both involving a photoinduced intramolecular rearrangement and the formation of a C−C bond.

1. Introduction

Sulfur-stabilized carbon radicals and carbanions often appear as reaction intermediates of great importance to synthetic chemistry. For instance, alpha-sulfoxide and sulfone carbanions are used in modern synthetic methodologies mediating many C−C bond forming reactions.[1] Gas-phase techniques allow for the direct observation of many of such species in their isolated form, while also permitting the characterization of their intrinsic properties and aiding the discovery of new reaction intermediates.

Dimethyl sulfoxide [DMSO, $CH_3S(O)CH_3$], like many polar organic molecules, exists in anionic form only as a dipole-bound anion,[2−5] where the excess electron is weakly bound in a diffuse orbital by virtue of the strong dipolar interaction. On the other hand, it is well-known that deprotonation of a stable parent molecule (M) can provide a binding site for the excess electron, producing base-type $[M-H]^-$ valence anions.[6] For instance, proton abstraction from DMSO forms the well-known dimethylsulfinyl carbanion (or dimsyl anion) $CH_3S(O)CH_2^-$. Numerous applications of this anionic species have been reported since its first observation by Corey and Chaykovsky highlighting its great synthetic capabilities.[7]

Theoretical[8,9] and experimental[10] studies on the dimsyl anion show that its excess charge is mostly localized on the carbon of the CH_2 segment. This additional electron is paired with a second valence electron in the hybridized nonbonding orbital of carbon. The anion possesses a pyramidal C−S(O)−C configuration, with an electron lone pair localized on the sulfur atom and a highly polarized S^+-O^- bond. Compared to neutral DMSO, where both S−C bonds are estimated to be 1.80 Å long, the S−CH_2 bond length of the anion is slightly compressed (1.72 Å), while the S−CH_3 bond is somewhat stretched (1.84 Å); see, for example, ref 9. Wolfe et al. attributed this effect to the stabilizing orbital interactions between the nonbonding electrons on the carbon atom and the orbitals of sulfur.[8] More recent work by Streitwieser and co-workers suggests that this effect may arise primarily from the electrostatic stabilization of the anionic carbon center in proximity to the positively charged S atom of the polarized sulfinyl group.[9,11] As a result of this unique structural arrangement, the potential tridenticity of this anion has been suggested based on possible O, S, and C nucleophilic reactivity.[12]

Despite the long standing interest in this anion, there are no reports on the $[M-2H]^-$ anions of DMSO. Reactions of the oxide radical anion O^- have proven to be a practical approach to synthesizing a variety of radical anions in the gas phase.[6,13] In addition to its ability for proton abstraction, O^- is also capable of abstracting H_2^+ (which stands for sequential abstraction of an H atom and a proton) from a wide range of molecules due to its high proton and hydrogen affinities.[13] In this study, we make use of this property to generate novel $[M-2H]^-$ anions of DMSO.

The resulting anionic species could be described as either carbene $CH_3S(O)CH^-$ or distonic $CH_2S(O)CH_2^-$ radical anions, depending on whether the O^- attack occurs on the hydrogens from a single carbon or from both carbon centers, respectively. The similar $CH_3C(O)CH^-$ and $CH_2C(O)CH_2^-$ anions have been observed upon formal 1,1 and 1,3 overall H_2^+ abstraction from neutral acetone by O^-, with some preference for the formation of the more stable oxyallyl anion $CH_2C(O)CH_2^-$.[14,15] The photoelectron imaging results presented in this work, in combination with a thorough analysis of the observed photofragments, suggest that the $CH_3S(O)CH^-$ anions are predominantly formed under our experimental conditions, with the excess electron residing in the out-of-plane carbon p orbital of the bent SCH segment.

Photodetachment from $CH_3S(O)CH^-$ reveals the carbene character of the remaining neutral. Carbenes are known reactive intermediates where the divalent carbon leads to low-lying singlet and triplet states. Although close in energy, these states

[†] Current address: Department of Chemistry, University of California, Santa Barbara, CA 93106-9510.

[‡] Current address: Department of Chemistry, University of California, Berkeley, CA 94720-1460.

10.1021/jp811323q CCC: $40.75
Published on Web 03/23/2009

exhibit noticeable differences in their chemical reactivity (see, for example, ref 16). Using photoelectron spectroscopy in combination with ab initio and density-functional calculations, we characterize the electronic structure of the $CH_3S(O)CH^-$ anion and the corresponding neutral. Photofragmentation experiments on this anion reveal two types of products, namely $HCSO^-$ and SO^-. While direct S−C bond cleavage is believed responsible for the $HCSO^-$ fragments, a photoinitiated intramolecular C−C bond formation is proposed as a likely mechanism for the SO^- channel. The effect of monohydration on this anion is also studied by examining the photoelectron spectra as well as the fragmentation patterns of the $CH_3S(O)CH^-\cdot H_2O$ ionic complex.

2. Experimental Setup

The experiments are carried out on mass-selected negative ions using a tandem time-of-flight (TOF) mass spectrometer[17] equipped with a velocity-mapped[18] imaging[19] assembly for detection of photoelectrons, as described previously.[20] The anions are formed by bubbling 10−20 psi of neat N_2O gas through a reservoir containing liquid dimethyl sulfoxide (Alfa Aesar 99+ %). The resulting gaseous mixture is expanded into vacuum through a 50 Hz pulsed nozzle (General Valve Series 99) and impacted with a 1 keV electron beam. Dissociative attachment of slow secondary electrons to neutral nitrous oxide yields precursor O^- radicals. According to the proposed mechanism, O^- then abstracts H_2^+ from neutral DMSO to generate the $[M-2H]^-$ anion plus an H_2O molecule. Water trapped within the gas delivery lines serves as an additional source of H_2O for the formation of anionic hydrates. The formation of these ions is experimentally challenging because of the low vapor pressure of DMSO and its tendency to adhere to surfaces.

The anions are pulse-extracted into a Wiley−McLaren[21] TOF mass spectrometer and monitored using an in-line microchannel plate (MCP) detector (Burle, Inc.) mounted at the end of the flight tube. Mass-selected ions are interrogated with a pulsed laser beam. The harmonics of a nanosecond Nd:YAG laser (Spectra Physics, Inc., Quanta-Ray LAB 130-50) provide 532, 355, and 266 nm pulses of about 30, 15, and 5 mJ/pulse respectively. The laser beam is mildly focused at the intersection with the ion beam using a 2 m focal length lens located 1.7 m before the interaction region.

Anionic photofragments are analyzed using a linear reflectron mass spectrometer and refocused on an off-axis MCP detector (Burle, Inc.) that collects the fragments 355° from the main ion beam trajectory.[17,20,22] The photofragment mass spectra are captured by a digitizing oscilloscope, averaged over ∼500 laser shots, and transferred to a computer. Photoelectron images are recorded in the direction perpendicular to the primary ion and laser beams. A 40 mm diameter MCP detector coupled to a P43 phosphor screen (Burle, Inc.) is mounted at the end of the μ-metal shielded electron flight tube. To discriminate against background, the MCPs are pulsed on for a 200 ns window timed with the arrival of the photoelectrons. Photoelectron images are captured by a CCD camera (Dalsa, Inc.), accumulated for 50 000 experimental cycles and transferred to a computer for storage and analysis. The O^- photoelectron spectrum is used for electron kinetic energy calibration.[23,24]

3. Results

3.a. Parent-Ion Mass Spectrum. A representative parent-ion mass spectrum is shown in Figure 1. In addition to the anticipated anions formed by expansion of N_2O gas with a small amount of H_2O present in the gas line,[25−27] the observed peaks at m/z = 76, 94, and 112 suggest a hydration series for the m/z = 76 anion, assigned as the $[M-2H]^-$ negative ion of DMSO and described throughout this work as $CH_3S(O)CH^-$. Other anions formed from DMSO include SO^-, small amounts of $HCSO^-$, and $NO^-\cdot$DMSO corresponding to m/z = 48, 61, and 108, respectively. Although the m/z = 94 peak may also correspond to the $CH_3S(O_2)CH_3^-$ anion resulting from the addition reaction of the atomic oxygen anion with DMSO, the photoelectron images presented below show no evidence that this compound is formed.

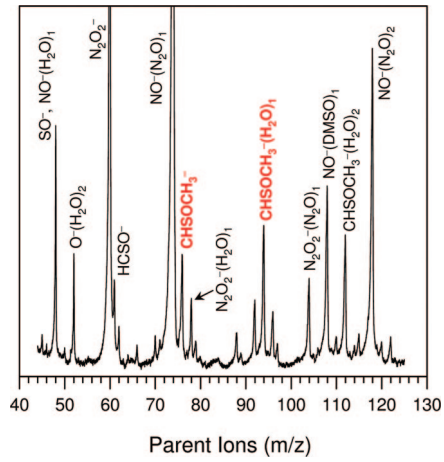

Figure 1. Representative mass spectrum displaying the anions formed by electron impact on the N_2O/DMSO gas mixture.

The spectrum in Figure 1 gives no indication of the formation of the dimsyl anion, $CH_3S(O)CH_2^-$. This is surprising, as atomic oxygen is sufficiently basic to deprotonate DMSO. The absence of the dimsyl anion must be at least partially due to the presence of water in our system, as we observed a similar effect in experiments with acetonitrile, where both H_2CCN^- and $HCCN^-$ were present in the absence of water, while only the $HCCN^-(H_2O)_n$ clusters were observed with the addition of water.[28]

3.b. Photoelectron Imaging. Figure 2 (left) shows the photoelectron images obtained for the $CH_3S(O)CH^-$ anion at 355 nm and for the $CH_3S(O)CH^-\cdot H_2O$ ionic complex at 266 nm. The images were acquired under the same electrostatic focusing conditions, and their corresponding energy spectra are plotted in the right of the figure as functions of electron binding energy (eBE). The photoelectron spectra and angular distributions reflected in the images were analyzed using the Reisler group's BASEX program.[29]

Three transitions are observed in each case shown in Figure 2, corresponding to the different rings on the photoelectron images and the resultant bands in the spectra. The numbers in parentheses shown next to the individual spectral bands are the corresponding photoelectron anisotropy parameter (β) values.

The highest-eBE band in the 355 nm $CH_3S(O)CH^-$ spectrum in Figure 2c is cut off at the photon energy limit (3.49 eV). We have therefore included an additional spectrum of this band shown as a dashed line in Figure 2c, extracted from a photoelectron image (not shown) acquired at 266 nm. From the 266 nm spectrum, the vertical detachment energy (VDE) corresponding to the high-eBE $CH_3S(O)CH^-$ band is estimated at 3.48 eV. The rest of the 266 nm trace overlaps well with the 355 nm spectrum and is therefore not shown.

The 355 nm $CH_3S(O)CH^-$ spectrum in Figure 2c was fitted using the sum of three Gaussian-type functions.[20] The peak

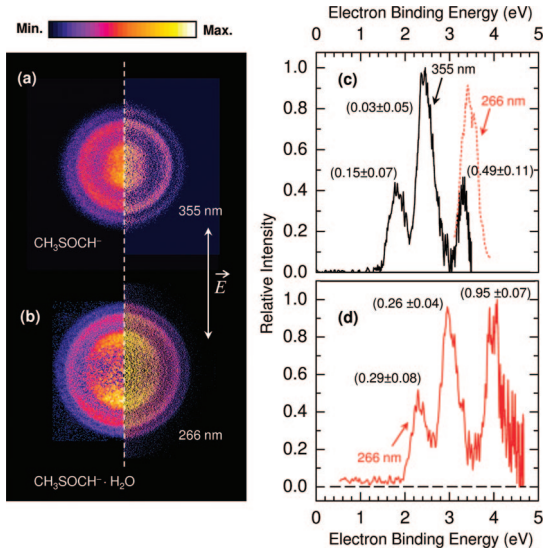

Figure 2. (a), (b) Photoelectron images and (c), (d) corresponding energy spectra for the $CH_3S(O)CH^-$ and $CH_3S(O)CH^- \cdot H_2O$ anions. The double arrow in (a) and (b) indicates the laser polarization direction. The numbers in parentheses (with error bars) in (c) and (d) are the anisotropy parameters determined for each of the corresponding spectral bands.

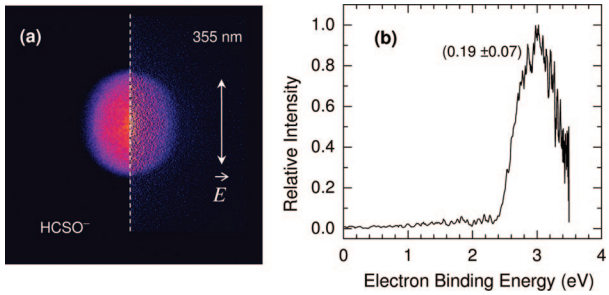

Figure 3. (a) 355 nm photoelectron image and (b) corresponding spectrum for the $HCSO^-$ anion. The double arrow in (a) indicates the laser polarization direction. The number in parentheses (with error bars) is the anisotropy parameter determined for the observed detachment band.

positions for these individual Gaussians are interpreted as the VDE values for the corresponding transitions: 1.79, 2.47, and 3.48 eV, respectively. In Section 4.b, we assign the lowest-eBE band to the ground singlet electronic state (S_0) of the remaining neutral $CH_3S(O)CH$ and the second band to the lowest triplet state, T_1, and the high-eBE band is tentatively assigned to an excited singlet, S_1.

From the 266 nm spectrum of the monohydrated anion shown in Figure 2d, we observe that each of the three bands is shifted to higher binding energies by 0.54 ± 0.05 eV with respect to the bare anion. The shift is attributed to the stabilization interaction between the anion and the solvent H_2O molecule. Because of the direct one-to-one correspondence of the transitions observed for the bare and monohydrated species, we conclude that no $CH_3S(O_2)CH_3^-$ anions, which have the same m/z ratio as $CH_3S(O)CH^- \cdot H_2O$, are formed in our experiment.

Figure 3a shows the 355 nm photoelectron image of $HCSO^-$, which corresponds to the relatively small peak in the parent-ion mass spectrum at $m/z = 61$. The VDE of this anion, determined as the eBE associated with the maximum of a Gaussian fit to the photoelectron band, is 2.97 eV with a full width at half-maximum of 0.8 eV. Characterization of this anion is relevant to the understanding of the photodissociation channels discussed in the next section, since methyl elimination from

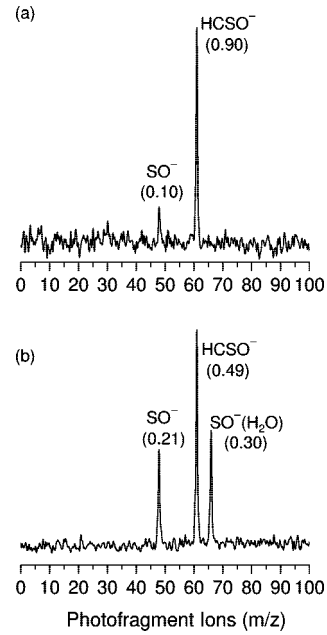

Figure 4. Photofragment mass spectra obtained at 532 nm for the (a) $CH_3S(O)CH^-$ and (b) $CH_3S(O)CH^- \cdot H_2O$ parent anions. The numbers in parentheses indicate the relative yields for the different fragments.

$CH_3S(O)CH^-$ results in the $HCSO^-$ product. Our calculations suggest that the anion responsible for the spectrum in Figure 3 has a singlet ground state. In good agreement with the experimental observations, the VDE estimated at the B3LYP/aug-cc-pVTZ level is 2.87 eV for the trans-isomer and 3.19 eV for the cis-configuration, the later being more stable by <0.1 eV at this level of theory. The $HCSO^-$ photoelectron spectrum in Figure 3 is significantly different from that reported for the $CH_3CH_2S^-$ anion,[30] also of $m/z = 61$, ruling out the possibility of this latter anion contributing to the peak observed in the parent-ion mass spectrum.

3.c. Photofragment Mass Spectra. Reported in Figure 4 are the anionic photofragment mass spectra obtained with 532 nm (2.32 eV) photoexcitation of the $CH_3S(O)CH^-$ and $CH_3S(O)CH^- \cdot H_2O$ anions. A dominant $HCSO^-$ ($m/z = 61$) photofragment peak is observed for both cases with additional contributions from SO^--based fragments. For the bare $CH_3S(O)CH^-$ anion, the $HCSO^-$ products account for about 90% of the total anionic fragmentation yield, while SO^- accounts for the remaining 10%. No anionic dissociation products were observed with 355 or 266 nm light. It is instructive to compare this result with the $CH_3C(O)CH^-$ anion formed from acetone, where a dominant fragmentation channel yielding $HCCO^-$ was observed by Lin and Grabowski.[14]

In comparison, the monohydrated anion $CH_3S(O)CH^- \cdot H_2O$ shows an enhanced yield of the SO^--based channel, including the $SO^- \cdot H_2O$ fragment, as evident in Figure 4b. The observation of the $SO^- \cdot H_2O$ photofragment suggests that the water molecule in the parent anionic complex binds to the sulfoxide group by means of hydrogen bonding to the oxygen atom. The combined yield of the SO^--based products from $CH_3SOCH^- \cdot H_2O$ accounts for about 51% of the anionic fragments yield, with the remaining 49% attributed to $HCSO^-$.

4. Discussion

4.a. Isomeric Structures. To aid the analysis of the experimental data, minimum-energy $C_2H_4SO^-$ structures were determined using the Gaussian 03 suite of programs.[31] The hybrid

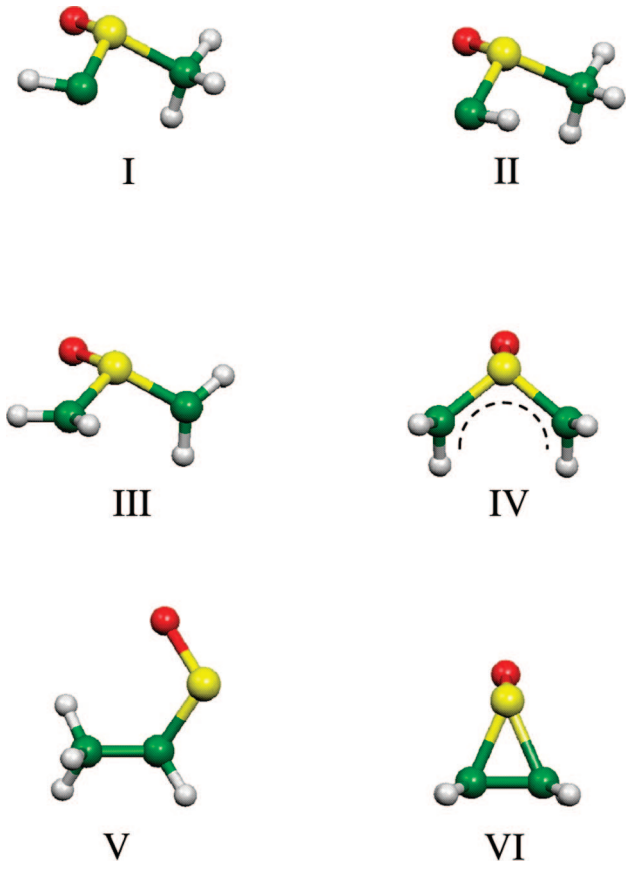

Figure 5. Structures for the $C_2H_4SO^-$ anions optimized at the UB3LYP/aug-cc-pVTZ level of theory.

B3LYP method was employed for most of the calculations shown in this work using the aug-cc-pVTZ basis set. In choosing the computational method, we performed extensive test calculations for the VDEs to the first singlet and triplet states of the corresponding neutrals for several well-characterized carbene anions, such as CH_2^-,[32,33] HCF^-, $HCCl^-$,[34–36] $HCNC^-$, and $HCCN^-$.[37] The B3LYP/aug-cc-pVTZ method proved to be on average within approximately ±0.25 eV of the reported experimental values. Calculations at the MP2 and CCSD(T) levels were consistent with the energetic orderings of the B3LYP predictions, varying only slightly in their respective relative energies.

The predicted potential minimum structures are displayed in Figure 5. No imaginary frequencies were found for these optimized geometries at the UB3LYP/aug-cc-pVTZ level of theory. Vertical detachment energies for the anions shown in Figure 5, corresponding to the low-lying singlet and triplet states of the neutrals, were determined from single-point energy calculations using the minimum energy geometries of the anions. The resulting single-point energies for the singlet or triplet neutral states are then compared to the ground state of the anion to obtain the VDEs shown in Table 1. Figure 6 displays a schematic diagram showing the calculated relative energies for the isomers shown in Figure 5 and their plausible correlations with the $HCSO^-$ and SO^- fragment channels.

We now focus on structure **I**, whose properties (as discussed in Sections 4b and 4c) best match the photoelectron spectrum shown in Figure 2c, and which is also consistent with the observed photofragments—in particular with formation of the $HCSO^-$ product. The optimized HC−S distance for structure **I** is 1.72 Å, the same as the H_2C−S distance for the dimsyl anion (1.72 Å from ref 9). This is an indication that no significant

TABLE 1: Relative Electronic Energies and Vertical Detachment Energies (VDE) for the Structures Shown in Figure 5 Obtained at the UB3LYP/aug-cc-pVTZ Level of Theory

		VDE (eV)	
structure	relative energy (eV)	singlet	triplet
I	0.0	1.967	2.522
II	0.114	2.026	2.573
III	0.056	2.486	2.400
IV	−0.037	2.270	2.525
V	−1.888	0.944	2.300
VI	−0.691	−0.353	
exptl		1.79 ± 0.02	2.47 ± 0.02

changes occur to the C−S bonding between these two anions. The extra electron in $CH_3S(O)CH^-$ occupies the empty out-of-plane orbital of the carbon atom in the CH segment. The Mulliken spin densities and charges, obtained from the UB3LYP calculations and shown in Figure 7, are consistent with this picture and additionally reveal the highly polarized S−O σ-bond, best described as S^+-O^-.[38] The S−O bond length in structure **I** of $CH_3S(O)CH^-$ is 1.55 Å, also similar to that of dimsyl. This is longer than 1.49 Å reported for the S−O bond distance of

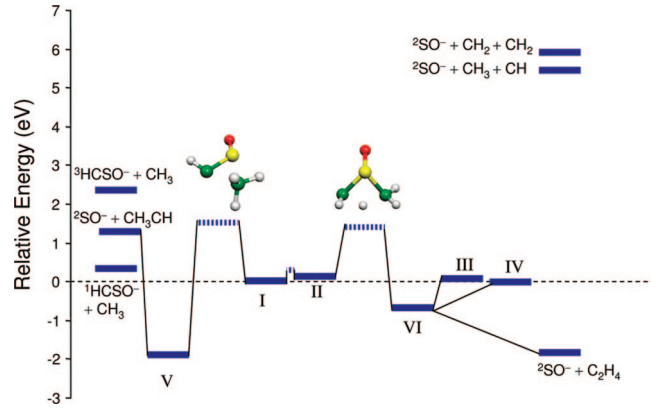

Figure 6. Schematic energy diagram showing some of the relevant stationary structures and fragment channel correlations, calculated at the UB3LYP/aug-cc-pVTZ level of theory. The equilibrium structures denoted by roman numerals are shown in Figure 5, while the corresponding relative energy values are summarized in Table 1.

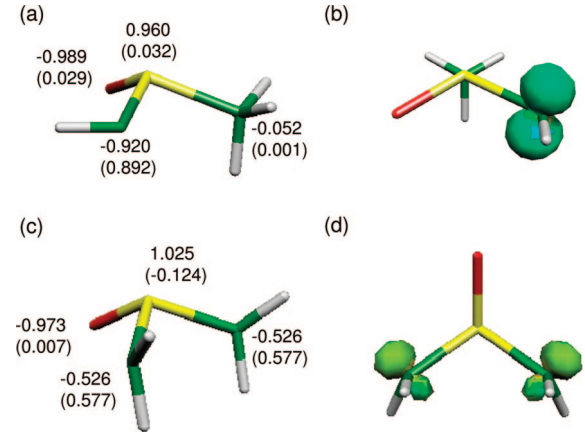

Figure 7. Mulliken charges with hydrogens summed into the C atoms and spin densities (in parentheses) for the carbene (a) $CH_3S(O)CH^-$ and distonic (c) $CH_2S(O)CH_2^-$ radical anions calculated at the UB3LYP/aug-cc-pVTZ level of theory. The contours in (b) and (d) are the $\alpha-\beta$ spin density plots for $CH_3S(O)CH^-$ and $CH_2S(O)CH_2^-$, respectively.

neutral DMSO (see, for example, ref 9). The Mulliken spin densities and charges for structure **IV** (the distonic radical anion) are also displayed in Figure 7, revealing that the excess electron is delocalized between the two carbon atoms while also preserving a pyramidal structure and a polarized S−O bond.

4.b. Photodetachment Transitions. Three main photoelectron bands are observed in the spectra shown in Figure 2. The predicted properties of structure **I** are in good agreement with these bands. For instance, the experimental VDEs for the first two bands in Figure 2c are 1.79 and 2.47 eV, respectively. These values are compared to the calculated VDEs of $CH_3S(O)CH^-$ (structure **I**) corresponding to the S_0 and T_1 states of the neutral: 1.97 and 2.52 eV, respectively (Table 1). The VDEs obtained with the anion reoptimized at the MP2/aug-cc-pVTZ level are 2.10 and 2.66 eV for the singlet and triplet transitions, respectively. The CCSD(T)/aug-cc-pVDZ calculations using this reoptimized MP2 structure give 1.75 eV as the VDE of the singlet band and 2.36 eV for the triplet.

Although the assignment of the photoelectron spectrum to structure **I** is reinforced by the observed photofragmentation products ($HCSO^-$, in particular), this assignment is not entirely unambiguous. First, the calculated VDEs of structures **I** and **II** are quite similar (see Table 1), while the barrier for the interconversion of isomer **I** into **II** by rotation about the CS bond is only ∼0.3 eV, as determined at the B3LYP/aug-cc-pVTZ level of theory. We nonetheless focus on isomer **I**, since it is predicted to be the more stable of the two species. The low thermal energy of the anionic beam and the short experimental time scales should preclude the anion formed by overall H_2^+ abstraction (structure **I** or structure **II**) from overcoming the larger energy barriers associated with the more stable structures displayed in Figure 6. Second, contributions from the symmetric $CH_2S(O)CH_2^-$ anion (structure **IV**) also cannot be ruled out completely based on the photoelectron spectra alone. While the spectra in Figure 2 show no distinct signatures for the coexistence of two different isomers, the predicted transitions for the distonic $CH_2S(O)CH_2^-$ anion are expected to fall in close proximity to the bands of structure **I**. Therefore, possible contributions of isomer **IV** could be disguised in the structureless bands of the photoelectron spectra. However, we emphasize again that structure **IV** is not easily reconciled with the formation of the observed $HCSO^-$ photofragments.

Returning to the photodetachment of CH_3SOCH^- (structure **I**), this process leaves either singlet or triplet electronic state carbenes. Our calculations suggest that the lowest-eBE band corresponds to removal of an electron from the singly occupied HOMO of the anion (out-of-plane p orbital), resulting in a neutral that can be viewed as a singlet carbene with two nonbonding paired electrons located on the in-plane sp^2-hybridized orbital of the divalent carbene center. Geometry optimization of this singlet neutral state reveals that the carbene is further stabilized by electron donation from the sulfur substituent into the empty p orbital of carbon, ultimately resulting in a planar C−S(O)−C skeleton with a much shorter HC−S bond (1.58 Å compared to 1.72 Å for the anion). The shortening of the bond is due to the additional π-C−S bonding. The adiabatic electron affinity (without zero-point vibrational energy correction) is estimated to be 1.18 eV at the B3LYP/aug-cc-pVTZ level of theory for detachment to the singlet state. The corresponding triplet state value is 2.08 eV. Experimental electron affinities are not reported here, since the large geometry distortions discussed above result in an unfavorable Franck−Condon overlap for the adiabatic transitions.

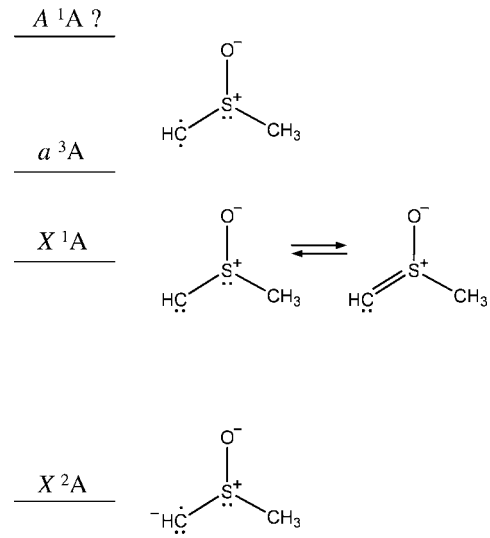

Figure 8. Schematic representation of the electronic states involved in the photodetachment of the $CH_3S(O)CH^-$ anion. The question mark next to $A\ ^1A$ reflects the uncertainty of this state's assignment.

The second band in the photoelectron spectra, assigned to the excited triplet (T_1) of the neutral, results from removal of a β-electron from the HOMO − 1 of the anion (the in-plane sp^2-hybridized orbital), leaving the carbene center in a triplet state. The geometry of the optimized triplet structure shows the most variation in the ∠SCH angle compared to that of the anion, opening from 105° to 123° according to our UB3LYP/aug-cc-pVTZ calculations. It is interesting that the geometry relaxation on the T_1 state does not result in a linear S−C−H configuration, as observed for the triplet states of HCCN and HCNC, where the π-electrons of the CN bond are potentially able to conjugate with both electrons on the HC fragment giving a quasilinear (or floppy) molecule.[37]

The third photoelectron band, with the highest binding energy, is tentatively assigned to an excited singlet state of the neutral, S_1. Excited state calculations for the singlet neutral molecule at the optimized geometry of the anion give excitation energies for the next singlet state of 1.99, 1.52, and 1.54 eV using the CIS/aug-cc-pVTZ, TD-B3LYP/aug-cc-pVTZ, and SAC-CI/6−311+G* levels of theory, respectively. Assuming that the first band is located at 1.80 eV (see Figure 2c), these results suggest that removal of an α-electron from the HOMO − 1 of the anion should result in photoelectrons in the range of eBE = 3.3−3.8 eV, which is consistent with the experimental data. However, the markedly positive anisotropy of this transition, contrasting the other two bands, is somewhat puzzling, hence the tentative nature of our assignment. Another possible interpretation involves the removal of an electron from the sulfur lone pair, which is expected to give positive anisotropy values.

A schematic representation of the proposed detachment transitions in $CH_3S(O)CH^-$ is shown in Figure 8. The spectrum recorded for the monohydrated anion shows that all three bands are shifted to higher binging energies by an equal amount (0.54 ± 0.05 eV), attributed to the stabilization induced on the anion by a solvent water molecule.

The accurate determination of the singlet−triplet energy gap is of crucial importance to carbene chemistry, and photoelectron spectroscopy of negative ions has proven to be the technique of choice for the experimental determination of this energy difference. Characterization of the singlet and triplet states of neutral carbenes by means of anion photodetachment has been reported previously by Lineberger and co-workers for several

systems, including CH_2^-,[32,33] CX_2^-, and halocarbene anions HCX^-, where X = halogen,[34−36] and the $HCCN^-$ and $HCNC^-$ isomeric anions.[37]

4.c. Photodissociation Mechanisms. Figure 6 displays a schematic reaction coordinate diagram showing the relative energies of the possible isomers and intermediates leading to the formation of the observed $HCSO^-$ and SO^- photofragments.

The $HCSO^-$ products are proposed to originate from direct S−C bond cleavage followed by methyl elimination from the $CH_3S(O)CH^-$ anion. The mechanism for SO^- production, however, is less clear, and several possible mechanisms are discussed below:

(i) Decomposition of $HCSO^-$ photofragments into SO^- + CH. A mechanism similar to the production of CO from $CH_3C(O)CH_3$, where predissociation of the CH_3CO photoproduct is viewed as the source of the observed carbonyl fragments.[39,40] Therefore, further decomposition of nascent $HCSO^-$ products is considered as a plausible mechanism for SO^- formation.

(ii) Concerted two-bond cleavage to give CH + SO^- + CH_3 fragments after absorption of a photon by $CH_3S(O)CH^-$ (or by the symmetric $CH_2S(O)CH_2^-$ anion to give SO^- + $2CH_2$). A recent study shows concerted bond breaking of DMSO upon UV excitation as a possible pathway for the production of SO + $2CH_3$.[41]

(iii) A 1,2-methyl migration from the sulfur atom to the carbene center forming a CH_3CHSO^- anion subsequently followed by an S−C bond cleavage that could result in CH_3CH + SO^- fragments—provided there is enough energy available in the excited system.

(iv) Cyclization into a $C_2H_4SO^-$ anion (structure **VI**) that undergoes fast decomposition into C_2H_4 + SO^-. Since neutral ethylene episulfoxide[42] is a well-known pyrolytic[43] and photolytic[44] source of SO, its anion is a possible source of SO^-. Formation of the cyclic intermediate may be preceded by an intramolecular C−H insertion in the electronically excited $CH_3S(O)CH^-$ anion or by promotion of C−C bonding in an excited electronic configuration of the $CH_2S(O)CH_2^-$ isomer.

Our calculations indicate that the $HCSO^-$ anion is more stable than the SO^- + CH fragments (this can be seen in Figure 6), arguing against mechanism i. In addition, no $HCSO^- \cdot H_2O$ photofragments were detected from $CH_3S(O)CH^- \cdot H_2O$. These photofragments would be expected if the observed $SO^- \cdot H_2O$ products were formed via mechanism i alone. Mechanism ii is also not very likely since there is not enough energy provided by the absorption of a single 532 nm photon to break two bonds simultaneously. A photoinitiated methyl migration, as suggested in mechanism iii, seems to be energetically accessible at this photon energy and therefore remains as a possible pathway in this discussion.

Mechanism iv is also highly favored based on energetic arguments. Similarly, Bowie et al. reported the observation of the HOS^- fragment in their mass spectra resulting from fragmentation of the $CH_3S(O)CH_2^-$ anion (dimsyl).[45] Their proposed mechanism involved proton transfer to oxygen, followed by a subsequent cyclization and elimination of the C_2H_4 olefin to give HOS^-.

One complication with mechanism iv is that the excess electron needs to vacate the out-of-plane p orbital of carbon for the C−H insertion to occur. One possible way to overcome this difficulty is having this electron transferred to the sulfoxide group. A similar argument applies for the $CH_2S(O)CH_2^-$ anion. Nonetheless, the poor electron affinity of cyclic ethylene episulfoxide does not favor the formation of a valence anion (as reflected by the negative VDE calculated for cyclic structure **VI**). The high dipole moment of the cyclic neutral (3.94 D at the UB3LYP/aug-cc-pVTZ level) suggests that a dipole-bound state may exist. Dipole-bound states can potentially act as doorways into dissociative valence states, as demonstrated by studies on nitromethane.[46] However, the formation of a long-lived dipole-bound structure is also unlikely in the present case, as such a state would be prone to autodetachment, because of the vibrational excitation likely imparted on the molecule during the process.

The observed enhancement in the SO^--based products upon hydration may be an indication of an increased electron affinity on the monohydrated cyclic intermediate. That is, stabilization of the excess electron by hydration is at the root of the enhanced abundance of SO^--based photoproducts. The smaller SO^- signal for the bare anion may then be thought of as resulting from the strong competition with delayed autodetachment. It also remains to be seen whether water could be lowering the reaction barrier to the fragmentation (as observed in other gaseous ions[47]) by participating in the rearrangement process.

The photofragmentation mechanisms presented here may be an incipient indication of the interesting synthetic and mechanistic properties of these anions. It would be worth examining their reactivity with nearby molecules and exploring their potential applications.

5. Summary

We have reported the observation of the $CH_3S(O)CH^-$ and $CH_3S(O)CH^- \cdot H_2O$ carbene anions. Photoelectron spectroscopy reveals singlet and triplet carbenes for the remaining neutral, with the singlet state assigned as the ground state. The proposed structure of the $CH_3S(O)CH^-$ ion is analogous to that of the well-known dimsyl anion $CH_3S(O)CH_2^-$, with the additional unpaired electron localized in the site of the missing H atom. Although formation of the distonic $CH_2S(O)CH_2^-$ radical anion is also expected, we found no conclusive evidence of the presence of this isomer. The photoelectron spectrum of $HCSO^-$ is also observed and reported for the first time in this work.

Two main types of anionic products found in 532 nm photofragmentation of $CH_3S(O)CH^-$ are a dominant $HCSO^-$ fragment, resulting from methyl elimination, and a less intense SO^- product. For the monohydrated anion, an additional $SO^- \cdot H_2O$ fragment is observed. Intriguingly, both the $SO^- \cdot H_2O$ and SO^- products are produced with much higher yields in the fragmentation of $CH_3S(O)CH^- \cdot H_2O$, compared to the SO^- yield from the dissociation of the bare $CH_3S(O)CH^-$ anion. Two possible pathways are proposed as likely mechanisms for the SO^--based photoproducts, both involving a photoinduced intramolecular rearrangement. One of the proposed mechanisms involves a methyl migration from sulfur to CH, forming a CH_3CHSO^- anion that is followed by C−S bond cleavage to give CH_3CH + SO^-. The other possibility involves a cyclic intermediate that quickly dissociates into C_2H_4 + SO^-.

Acknowledgment. We have benefited greatly from discussions with Dr. Daniel Goebbert. We are pleased to acknowledge support of the computational aspects of this work by the University of Arizona High Performance Computing Center. Financial support is provided by the National Science Foundation (grant CHE-0713880).

References and Notes

(1) Oae, S. a. U. Y. In *The Chemistry of Sulphones and Sulphoxides*; Patai, S. a. R. Z., Stirling, C., Eds.; John Wiley & Sons: Chichester, 1988; p 583.

(2) Carles, S.; Desfrancois, C.; Schermann, J. P.; Berges, J.; Houee-Levin, C. *Int. J. Mass Spectrom.* **2001**, *205*, 227.

(3) Desfrancois, C.; Abdoulcarime, H.; Schermann, J. P. *Int. J. Mod. Phys. B* **1996**, *10*, 1339.

(4) Hammer, N. I.; Diri, K.; Jordan, K. D.; Desfrancois, C.; Compton, R. N. *J. Chem. Phys.* **2003**, *119*, 3650.

(5) Hammer, N. I.; Hinde, R. J.; Compton, R. N.; Diri, K.; Jordan, K. D.; Radisic, D.; Stokes, S. T.; Bowen, K. H. *J. Chem. Phys.* **2004**, *120*, 685.

(6) Harrison, A. G. *Chemical Ionization Mass Spectrometry*, 2nd ed.; CRC Press: Boca Raton, FL, 1992.

(7) Corey, E. J.; Chaykovsky, M. *J. Am. Chem. Soc.* **1962**, *84*, 866.

(8) Wolfe, S.; Stolow, A.; Lajohn, L. A. *Tetrahedron Lett.* **1983**, *24*, 4071.

(9) Speers, P.; Laidig, K. E.; Streitwieser, A. *J. Am. Chem. Soc.* **1994**, *116*, 9257.

(10) Dozmorov, S. V. *J. Appl. Spectrosc.* **1986**, *45*, 957.

(11) Bors, D. A.; Streitwieser, A. *J. Am. Chem. Soc.* **1986**, *108*, 1397.

(12) Buncel, E.; Park, K. T.; Dust, J. M.; Manderville, R. A. *J. Am. Chem. Soc.* **2003**, *125*, 5388.

(13) Lee, J.; Grabowski, J. J. *Chem. Rev.* **1992**, *92*, 1611.

(14) Lin, M. X.; Grabowski, J. J. *Int. J. Mass Spectrom.* **2004**, *237*, 149.

(15) Dawson, J. H. J.; Noest, A. J.; Nibbering, N. M. M. *Int. J. Mass Spectrom.* **1979**, *30*, 189.

(16) Eisenthal, K. B.; Moss, R. A.; Turro, N. J. *Science* **1984**, *225*, 1439.

(17) Johnson, M. A.; Lineberger, W. C. Pulsed Methods for Cluster Ion Spectroscopy. In *Techniques for the Study of Ion Molecule Reactions*; Farrar, J. M., Saunders, W. H., Eds.; Wiley: New York, 1988; p 591.

(18) Eppink, A. T. J. B.; Parker, D. H. *Rev. Sci. Instrum.* **1997**, *68*, 3477.

(19) Chandler, D. W.; Houston, P. L. *J. Chem. Phys.* **1987**, *87*, 1445.

(20) Velarde, L.; Habteyes, T.; Sanov, A. *J. Chem. Phys.* **2006**, *125*, 114303.

(21) Wiley, W. C.; McLaren, I. H. *Rev. Sci. Instrum.* **1955**, *26*, 1150.

(22) Nadal, M. E.; Kleiber, P. D.; Lineberger, W. C. *J. Chem. Phys.* **1996**, *105*, 504.

(23) Valli, C.; Blondel, C.; Delsart, C. *Phys. Rev. A* **1999**, *59*, 3809.

(24) Cavanagh, S. J.; Gibson, S. T.; Gale, M. N.; Dedman, C. J.; Roberts, E. H.; Lewis, B. R. *Phys. Rev. A* **2007**, *76*, 052708.

(25) Coe, J. V.; Snodgrass, J. T.; Friedhoff, K. M.; Bowen, K. H. *J. Chem. Phys.* **1987**, *87*, 4302.

(26) Eaton, J. G.; Arnold, S. T.; Bowen, K. H. *Int. J. Mass Spectrom.* **1990**, *102*, 303.

(27) Velarde, L.; Habteyes, T.; Grumbling, E.; Pichugin, K.; Sanov, A. *J. Chem. Phys.* **2007**, *127*, 084302.

(28) Velarde, L. Ph.D. Dissertation, University of Arizona, 2008.

(29) Dribinski, V.; Ossadtchi, A.; Mandelshtam, V. A.; Reisler, H. *Rev. Sci. Instrum.* **2002**, *73*, 2634.

(30) Moran, S.; Ellison, G. B. *J. Phys. Chem.* **1988**, *92*, 1794.

(31) Frisch, M. J.; et al. *Gaussian 03*, Rev. B.01 ed.; Gaussian, Inc.: Wallingford, CT, 2004.

(32) Leopold, D. G.; Murray, K. K.; Lineberger, W. C. *J. Chem. Phys.* **1984**, *81*, 1048.

(33) Leopold, D. G.; Murray, K. K.; Miller, A. E. S.; Lineberger, W. C. *J. Chem. Phys.* **1985**, *83*, 4849.

(34) Schwartz, R. L.; Davico, G. E.; Ramond, T. M.; Lineberger, W. C. *J. Phys. Chem. A* **1999**, *103*, 8213.

(35) Murray, K. K.; Leopold, D. G.; Miller, T. M.; Lineberger, W. C. *J. Chem. Phys.* **1988**, *89*, 5442.

(36) Gilles, M. K.; Ervin, K. M.; Ho, J.; Lineberger, W. C. *J. Phys. Chem.* **1992**, *96*, 1130.

(37) Nimlos, M. R.; Davico, G.; Geise, C. M.; Wenthold, P. G.; Lineberger, W. C.; Blanksby, S. J.; Hadad, C. M.; Petersson, G. A.; Ellison, G. B. *J. Chem. Phys.* **2002**, *117*, 4323.

(38) Dobado, J. A.; Martinez-Garcia, H.; Molina, J. M.; Sundberg, M. R. *J. Am. Chem. Soc.* **1999**, *121*, 3156.

(39) Donaldson, D. J.; Leone, S. R. *J. Chem. Phys.* **1986**, *85*, 817.

(40) Liu, D.; Fang, W. H.; Fu, X. Y. *Chem. Phys. Lett.* **2000**, *325*, 86.

(41) Ho, J. W.; Chen, W. K.; Cheng, P. Y. *J. Am. Chem. Soc.* **2007**, *129*, 3784.

(42) Hartzell, G. E.; Paige, J. N. *J. Am. Chem. Soc.* **1966**, *88*, 2616.

(43) Saito, S. *Bull. Chem. Soc. Jpn.* **1969**, *42*, 667.

(44) Wu, F.; Chen, X. R.; Weiner, B. R. *J. Am. Chem. Soc.* **1996**, *118*, 8417.

(45) Bowie, J. H.; Stringer, M. B.; Hayes, R. N. *Rapid Commun. Mass Spectrom.* **1990**, *4*, 129.

(46) Sommerfeld, T. *Phys. Chem. Chem. Phys.* **2002**, *4*, 2511.

(47) Vohringer-Martinez, E.; Hansmann, B.; Hernandez, H.; Francisco, J. S.; Troe, J.; Abel, B. *Science* **2007**, *315*, 497.

JP811323Q